Experimental Validation of the Non-Orthogonal Serret–Frenet Parametrization Applied to the Path Following Task

Filip Dyba[a]

Department of Cybernetics and Robotics, Faculty of Electronics, Photonics and Microsystems, Wrocław University of Science and Technology, Janiszewskiego Street 11/17, Wrocław, 50-372, Poland

Keywords: Backstepping Integrator, KINOVA® Redundant Manipulator, Non-Orthogonal Projection, Path Following, Serret–Frenet Parametrization.

Abstract: The path following task belongs to the fundamental robotic tasks. It consists of following a spatial curve parametrized with a curvilinear distance. In this time-independent approach no time regimes are imposed on a robot. In fact, it is a natural definition of a task for many robots, e.g. autonomous vehicles. In the paper a path following algorithm based on the non-orthogonal Serret–Frenet parametrization is presented. Such an approach is global and does not introduce any constraints to the robot description with respect to the path. It has been extensively studied recently. Hence, an experimental verification of the algorithm is proposed. The validation was conducted on a laboratory test–bed equipped with a redundant manipulator — the KINOVA® *Gen3 Ultra lightweight robot*. In the paper a case study is proposed to compare simulation results and experimental measurements. It is an example how the mathematical legacy of the past centuries can be used for modern solutions. The experimental study confirms the practical suitability of the presented control algorithm.

1 INTRODUCTION

The path following task is one of the basic robotic tasks distinguished in the literature and is a common task in many contemporary applications. It seems to be a natural solution to the encountered problems in modern robotics, e.g. it is eagerly used to control autonomous vehicles (Rokonuzzaman et al., 2021; Encarnação and Pascoal, 2000). Moreover, researchers have successfully harnessed the idea of path tracking for some non-obvious applications, such as controlling flying robots (Lugo-Cárdenas et al., 2017) or mobile manipulators (Mazur and Szakiel, 2009). Hence, in the paper the next step in the development of the path following algorithms, namely the experimental validation, is presented.

According to (Hung et al., 2023), the task is to force a robot to approach and move along a geometrical curve (path) defined in its workspace, whereas a velocity profile along the path has to be asymptotically tracked. A path is a purely geometrical description of a motion. It means that no time regimes are imposed on a controlled robot. The lack of time dependency is particularly vital in applications with control constraints. It is a clear advantage in comparison with some time-dependent approaches, such as the trajectory tracking problem (Mazur and Cholewiński, 2016).

In the literature different approaches to the path description can be met, namely the parametric methods (Mazur and Płaskonka, 2012; Liao et al., 2015) and the non-parametric techniques (Morro et al., 2011; Michałek and Gawron, 2018). The first approach is focused on a geometrical description of a robot with respect to a moving reference object, while the second one is a purely numerical analysis of shapes and surfaces. In the paper the parametric approach is experimentally verified as it has been eagerly considered in many applications, both on the plane (Micaelli and Samson, 1993; Płaskonka, 2013; Domski and Mazur, 2018) and in the three-dimensional space (Mazur et al., 2015; Cholewiński and Mazur, 2019).

The most frequently considered curvilinear parametrization method is the Serret–Frenet parametrization. It allows one to describe a robot with respect to a curve. In order to do so, a robot's guidance point needs to be projected onto the path.

[a] https://orcid.org/0000-0001-9202-519X

Dyba, F.
Experimental Validation of the Non-Orthogonal Serret-Frenet Parametrization Applied to the Path Following Task.
DOI: 10.5220/0012164200003543
In *Proceedings of the 20th International Conference on Informatics in Control, Automation and Robotics (ICINCO 2023) - Volume 1*, pages 608-615
ISBN: 978-989-758-670-5; ISSN: 2184-2809

Two approaches are distinguished: orthogonal and non-orthogonal. The orthogonal projection (Dyba and Mazur, 2023) is valid only locally and requires finding the shortest distance between the controlled robot and the path. In contrary, the non-orthogonal projection is a global method. Although it requires considering more control variables, it does not introduce any additional constraints.

Due to that facts, the non-orthogonal Serret–Frenet parametrization has been intensively investigated (Mazur and Dyba, 2023). The algorithm has been designed with the usage of the backstepping integrator method (Krstić et al., 1995), because of the cascaded structure of the system.

In the paper an experimental validation of the theoretically designed algorithm is presented. The simulation study is validated with experiments on a test–bed consisting of the KINOVA® *Gen3 Ultra lightweight robot*. The gathered measurements are compared in order to evaluate the practical usefulness of the proposed control algorithm.

2 Serret–Frenet PARAMETRIZATION

The most popular curvilinear parametrization was defined in 19th century by Serret and Frenet. It is eagerly used in many contemporary applications in various fields such as mathematics, physics, computer graphics and also in robotics. This parametric description of a curve defines a local frame consisting of three unit vectors: tangent to a curve $\boldsymbol{T}$, normal to a curve $\boldsymbol{N}$, and binormal to a curve $\boldsymbol{B}$. They span an orthonormal basis in $\mathbb{R}^3$. The Serret–Frenet frame, which is also frequently called the Frenet trihedron, describes the curve geometry locally. Its visualization is presented in Fig. 1. The base vectors of the Serret–

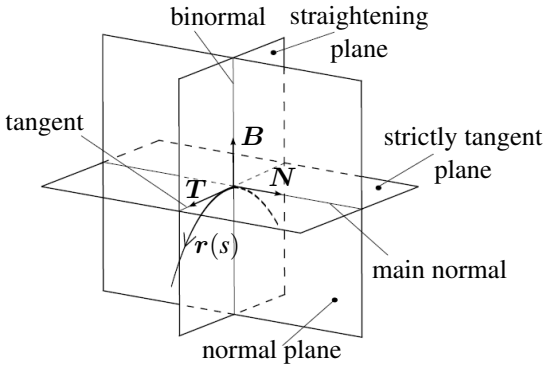

Figure 1: Frenet trihedron.

Frenet frame are defined as follows (Oprea, 2007)

$$\boldsymbol{T}(s) = \frac{\mathrm{d}\boldsymbol{r}(s)}{\mathrm{d}s}, \tag{1a}$$

$$\boldsymbol{N}(s) = \frac{\frac{\mathrm{d}\boldsymbol{T}(s)}{\mathrm{d}s}}{\left\| \frac{\mathrm{d}\boldsymbol{T}(s)}{\mathrm{d}s} \right\|}, \tag{1b}$$

$$\boldsymbol{B}(s) = \boldsymbol{T}(s) \times \boldsymbol{N}(s), \tag{1c}$$

where $\boldsymbol{r}(s)$ is the analytical description of a curve in $\mathbb{R}^3$, and s is the so-called curvilinear distance. The s parameter should be understood as the distance from the assumed initial point of a curve to the current point. Its value is equal to the length of a string placed precisely along a curve (Dyba and Mazur, 2023).

The evolution of the Serret–Frenet frame fully describes the geometry of a curve. Let us define a rotation matrix which consists of base vectors spanning Frenet trihedron, i.e.

$$\boldsymbol{S}(s) = \begin{bmatrix} \boldsymbol{T}(s) & \boldsymbol{N}(s) & \boldsymbol{B}(s) \end{bmatrix}, \tag{2}$$

$\boldsymbol{S} \in \mathbb{SO}(3)$ (Selig, 2005). Then, the frame evolution is expressed with the equation (Oprea, 2007)

$$\frac{\mathrm{d}\boldsymbol{S}(s)}{\mathrm{d}s} = \begin{bmatrix} \boldsymbol{T}^T(s) \\ \boldsymbol{N}^T(s) \\ \boldsymbol{B}^T(s) \end{bmatrix}^T \begin{bmatrix} 0 & -\kappa(s) & 0 \\ \kappa(s) & 0 & -\tau(s) \\ 0 & \tau(s) & 0 \end{bmatrix} = \boldsymbol{S}(s)\boldsymbol{W}(s), \tag{3}$$

where κ is the curvature (the curve swerve from a straight line), τ is the torsion (the curve swerve from a plane), and $\boldsymbol{W}$ is the antisymmetric matrix, i.e. $\boldsymbol{W} = -\boldsymbol{W}^T$. It should be emphasized that the frame evolution directly depends on the geometrical invariants κ and τ, which are defined as (Mazur et al., 2015)

$$\kappa(s) = \left\| \frac{\mathrm{d}\boldsymbol{T}(s)}{\mathrm{d}s} \right\|, \tag{4a}$$

$$\tau(s) = \frac{1}{\kappa^2(s)} \left\langle \frac{\mathrm{d}\boldsymbol{r}(s)}{\mathrm{d}s} \times \frac{\mathrm{d}^2\boldsymbol{r}(s)}{\mathrm{d}s^2}, \frac{\mathrm{d}^3\boldsymbol{r}(s)}{\mathrm{d}s^3} \right\rangle, \tag{4b}$$

where $\langle \cdot, \cdot \rangle$ denotes a scalar product of vectors.

3 MATHEMATICAL MODEL OF A ROBOT

In the paper a holonomic stationary manipulator is taken into account. It is assumed that it is a redundant robot. Hence, it has more than six degrees of freedom, i.e. $\boldsymbol{q} \in \mathbb{R}^n$, $n > 6$, where $\boldsymbol{q}$ is the vector of the manipulator configuration consisting of joint positions.

The position of the end-effector in the base frame may be calculated according to the forward kinematics task (Spong and Vidyasagar, 1991)

$$\boldsymbol{p} = k(\boldsymbol{q}) \in \mathbb{R}^3. \tag{5}$$

The position $\boldsymbol{p}$ will be referred to as the robot guidance point. The end-effector velocities may be calculated from the equation

$$\begin{pmatrix} \dot{\boldsymbol{p}} \\ \boldsymbol{\omega} \end{pmatrix} = \boldsymbol{J}(\boldsymbol{q})\dot{\boldsymbol{q}} = \begin{bmatrix} \boldsymbol{J}_v(\boldsymbol{q}) \\ \boldsymbol{J}_{\boldsymbol{\omega}}(\boldsymbol{q}) \end{bmatrix} \dot{\boldsymbol{q}}, \tag{6}$$

where $\dot{\boldsymbol{p}}$ is the linear velocity of the end-effector, $\boldsymbol{\omega}$ is its angular velocity, and $\boldsymbol{J}(\boldsymbol{q}) \in \mathbb{R}^{6\times n}$ is the Jacobi matrix which consists of submatrices $\boldsymbol{J}_v, \boldsymbol{J}_{\boldsymbol{\omega}} \in \mathbb{R}^{3\times n}$ corresponding to transformations to linear and angular velocities, respectively. In the following sections only the end-effector position and its linear velocity will be considered. Hence, let us define the matrix $\boldsymbol{J}_v$

$$\boldsymbol{J}_v(\boldsymbol{q}) = \frac{\partial k(\boldsymbol{q})}{\partial \boldsymbol{q}}. \tag{7}$$

Dynamics of the manipulator is derived with the usage of the Lagrange formalism (Siciliano and Khatib, 2007) and the model is expressed as

$$\boldsymbol{M}(\boldsymbol{q})\ddot{\boldsymbol{q}} + \boldsymbol{C}(\dot{\boldsymbol{q}},\boldsymbol{q})\dot{\boldsymbol{q}} + \boldsymbol{D}(\boldsymbol{q}) = \boldsymbol{u}, \tag{8}$$

where $\boldsymbol{M}(\boldsymbol{q}) \in \mathbb{R}^{n\times n}$ defines the inertia matrix, $\boldsymbol{C}(\dot{\boldsymbol{q}},\boldsymbol{q}) \in \mathbb{R}^{n\times n}$ is the matrix of Coriolis and centrifugal forces, $\boldsymbol{D}(\boldsymbol{q}) \in \mathbb{R}^n$ is the vector of gravity terms, and $\boldsymbol{u} \in \mathbb{R}^n$ denotes the generalized control forces applied to respective joints. In the model (8) other dynamics effects, such as friction, are neglected.

3.1 Robot Equations with Respect to a Path

In order to describe a robot with respect to a path, understood as a curve in $\mathbb{R}^3$ space, the robot guidance point P has to be projected onto the path. To do so, the non-orthogonal projection may be harnessed. Such a method is a global procedure and it does not introduce any singularities in the robot description. The point projected onto a path P' may be at any distance from the guidance point P, i.e. it may be located ahead of the point P or behind it during the robot motion. The point P' is at a distance s from the initial point of the curve, so it is also the origin point of the Serret–Frenet frame associated with the path. The idea of the non-orthogonal projection is presented in Fig. 2. The $X_0Y_0Z_0$ frame is the global reference frame which is identified with the manipulator base frame.

According to the notation in Fig. 2, the position of the robot guidance point with respect to the local Serret–Frenet frame is defined as

$$\boldsymbol{d} = \boldsymbol{S}^T(\boldsymbol{p}-\boldsymbol{r}) = \begin{pmatrix} d_1 & d_2 & d_3 \end{pmatrix}^T. \tag{9}$$

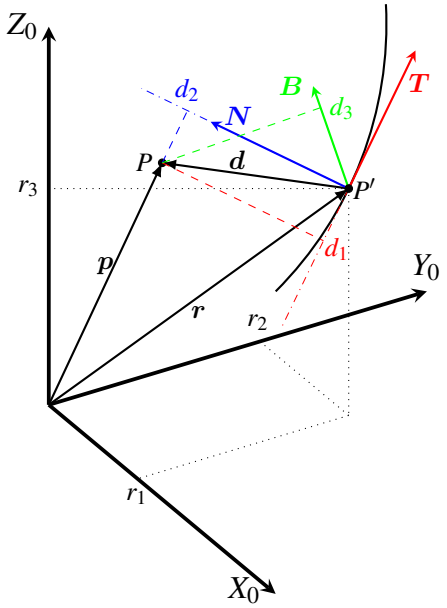

Figure 2: Non-orthogonal projection of the robot guidance point P onto the curve $\boldsymbol{r}$.

The robot kinematics with respect to the path is derived by differentiating equation (9)

$$\dot{\boldsymbol{d}} = \boldsymbol{S}^T(\dot{\boldsymbol{p}} - \dot{\boldsymbol{r}}) + \dot{\boldsymbol{S}}^T(\boldsymbol{p}-\boldsymbol{r}). \tag{10}$$

Let us notice that the element $\boldsymbol{S}^T\dot{\boldsymbol{r}}$ defines the linear velocity of the point P' in the Serret–Frenet reference frame. Hence, the following relation holds

$$\boldsymbol{S}^T\dot{\boldsymbol{r}} = \begin{pmatrix} \left\langle \boldsymbol{T}, \frac{\mathrm{d}\boldsymbol{r}}{\mathrm{d}s} \right\rangle \\ \left\langle \boldsymbol{N}, \frac{\mathrm{d}\boldsymbol{r}}{\mathrm{d}s} \right\rangle \\ \left\langle \boldsymbol{B}, \frac{\mathrm{d}\boldsymbol{r}}{\mathrm{d}s} \right\rangle \end{pmatrix} \dot{s} \overset{(1a)}{=} \begin{pmatrix} \dot{s} \\ 0 \\ 0 \end{pmatrix}. \tag{11}$$

Moreover, it is true that

$$\dot{\boldsymbol{S}}^T(\boldsymbol{p}-\boldsymbol{r}) = \dot{s}\frac{\mathrm{d}\boldsymbol{S}^T}{\mathrm{d}s}(\boldsymbol{p}-\boldsymbol{r}) \overset{(3)}{=} \dot{s}(\boldsymbol{S}\boldsymbol{W})^T(\boldsymbol{p}-\boldsymbol{r}) = \\ = -\dot{s}\boldsymbol{W}\boldsymbol{S}^T(\boldsymbol{p}-\boldsymbol{r}) \overset{(9)}{=} -\dot{s}\boldsymbol{W}\boldsymbol{d}. \tag{12}$$

As a result, equation (10) is reformulated taking into account equations (6), (11) and (12)

$$\dot{\boldsymbol{d}} = \boldsymbol{S}^T\boldsymbol{J}_v\dot{\boldsymbol{q}} - \begin{pmatrix} \dot{s} \\ 0 \\ 0 \end{pmatrix} - \dot{s}\boldsymbol{W}\boldsymbol{d} = \boldsymbol{L}\dot{\boldsymbol{q}} + \boldsymbol{F}, \tag{13}$$

where $\boldsymbol{L} = \boldsymbol{S}^T\boldsymbol{J}_v \in \mathbb{R}^{3\times n}$, and $\boldsymbol{F} \in \mathbb{R}^3$.

4 CONTROL PROBLEM FORMULATION

The control problem is to enforce the motion of the manipulator end-effector along a spatial path defined in the robot workspace.

The following assumptions are made:

- the desired path is defined as a pure geometrical object in $\mathbb{R}^3$ space;
- the Serret–Frenet frame is well-defined in every point of the path, so the curve is at least of $\mathcal{C}^3$ class and has no zero-curvature points;
- the desired velocity profile of the Serret–Frenet frame along the path is defined arbitrarily and tracked during the manipulator motion;
- the considered manipulator is stationary, holonomic and redundant;
- the manipulator kinematics is precisely known and the robot operates outside the singular configurations;
- parameters of the manipulator dynamics may remain unknown;
- only control of the end-effector position is considered.

It is worth noticing that tracking of the desired velocity profile along the path is a secondary subproblem. The profile defines the motion of the Serret–Frenet frame and does not violate the geometrical description of the path. It may be freely tuned regarding the robot limitations.

It may be observed that the full model of the manipulator for the path following task consists of two groups of equations:

1. Robot description with respect to the desired path given by equation (13). That equation defines constraints resulting from the desired motion along the path. The structure resembles the 1st order velocity constraints characteristic of nonholonomic systems.
2. Manipulator dynamics given by equation (8).

The kinematic motion along the path cannot be performed directly, but only by taking into account the manipulator dynamics. Thus, it is clear that the system has a cascade structure.

As a result, the backstepping integrator approach (Krstić et al., 1995) may be used for the control law design. The control cascade consists of two stages:

1. Kinematic controller $\dot{\boldsymbol{q}}_{ref}$: generates reference velocity profiles as though the dynamical part of the model did not exist. The velocity profiles have to satisfy constraints resulting from the desired path, i.e. they guarantee motion of the end-effector along the path by reducing the path following error $\boldsymbol{e_d}$ to zero, $\boldsymbol{e_d} \to \boldsymbol{0}$.
2. Dynamic controller $\boldsymbol{u}$: the reference velocity profiles cannot be performed directly on the manipulator due the cascade structure. As a consequence, a dynamic controller is required to follow the profiles generated on the previous level of the cascade. Hence, the velocity profile following error $\dot{\boldsymbol{e}}_{\boldsymbol{q}}$ is defined.

A schematic view of the full control system is presented in Fig. 3.

4.1 Control Law

For the defined control system, the following kinematic controller is proposed

$$\dot{\boldsymbol{q}}_{ref} = \boldsymbol{L}^{\#}(\dot{\boldsymbol{d}}_d - \boldsymbol{K}_k \boldsymbol{e_d} - \boldsymbol{F}), \tag{14}$$

where $\boldsymbol{d}_d$ is the desired position with respect to the Serret–Frenet frame, $\boldsymbol{e_d} = \boldsymbol{d} - \boldsymbol{d}_d$ is the path following error, $\boldsymbol{K}_k$ is the positive-definite matrix, and # denotes the Moore–Penrose pseudoinverse, i.e. $\boldsymbol{L}^{\#} = \boldsymbol{L}^T(\boldsymbol{L}\boldsymbol{L}^T)^{-1}$ holds. In the closed feedback loop the system (13) is described by the equation

$$\dot{\boldsymbol{e}}_{\boldsymbol{d}} + \boldsymbol{K}_k \boldsymbol{e_d} = \boldsymbol{0}, \tag{15}$$

which is clearly asymptotically stable with zero equilibrium point for the positive-definite matrix $\boldsymbol{K}_k$. Thus, the control law (14) meets the imposed requirements.

The velocity profile following error $\dot{\boldsymbol{e}}_{\boldsymbol{q}}$ considered on the second stage of the control cascade is coupled with the path following error $\boldsymbol{e_d}$ and directly depends on the error signal defined for the first stage of the control cascade

$$\dot{\boldsymbol{e}}_{\boldsymbol{q}}(\boldsymbol{e_d}) = \dot{\boldsymbol{q}} - \dot{\boldsymbol{q}}_{ref} = \dot{\boldsymbol{q}} - \boldsymbol{L}^{\#}(\dot{\boldsymbol{d}}_d - \boldsymbol{K}_k \boldsymbol{e_d} - \boldsymbol{F}). \tag{16}$$

For the second stage of the control cascade the dynamical PD controller, called the adaptive λ-tracking algorithm, is used. The algorithm was introduced in (Mazur and Schmid, 2000) and is defined by the following equation

$$\boldsymbol{u} = -K(t)\boldsymbol{E}(t), \tag{17}$$

where $\boldsymbol{E}(t) = \boldsymbol{K}_d \dot{\boldsymbol{e}}_{\boldsymbol{q}}(t) + \boldsymbol{K}_p \boldsymbol{e}_{\boldsymbol{q}}(t)$, $\boldsymbol{K}_d = \mathrm{diag}\{K_{d_i}\}$, $\boldsymbol{K}_p = \mathrm{diag}\{K_{p_i}\}$ are positive-definite matrices, $i = 1, \ldots, n$, and the coefficient K is the gain which adaptation is defined as

$$\dot{K}(t) = \begin{cases} (\|\boldsymbol{E}(t)\| - \lambda) \cdot \|\boldsymbol{E}(t)\|, & \|\boldsymbol{E}(t)\| > \lambda, \\ 0, & \|\boldsymbol{E}(t)\| \leq \lambda, \end{cases} \tag{18}$$

where $\lambda > 0$ is the arbitrarily chosen radius of the dead zone, in which the adaptive gain is not increased.

The λ - tracking algorithm guarantees that the error signals are limited. In contrary to the classical PD control law (Qu and Dorsey, 1991), the values of the error bounds explicitly depend on the chosen control gains, which is a significant advantage. According to (Mazur and Schmid, 2000), the velocity profile

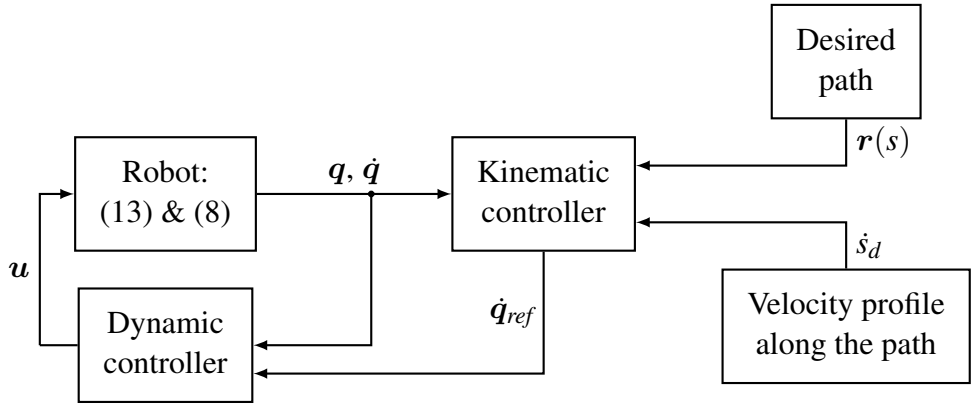

Figure 3: Scheme of the cascaded control system.

following errors $\dot{e}_q$ converge in the limit to a ball centred at $\mathbf{0}$. The ball radius for the i-th element of the vector $\dot{e}_q$ is equal to the value of $2\lambda/K_{d_i}$.

Hence, the dynamic control law (17) guarantees that the velocity profile following errors converge to the predefined regions. As a consequence, the required precision for the velocity profile tracking is assured and the path is satisfactory followed.

It is noteworthy that the presented dynamic control law may be applied when the structure of the manipulator dynamics is completely unknown. The controller (17) does not require any knowledge of the parameters of the model (8).

5 CASE STUDY

The theoretical deliberations were verified with both simulation and experimental studies[1]. In this section the achieved results are compared.

The simulation study was conducted with the MATLAB and SIMULINK environments. The experimental test–bed used for the validation consisted of the KINOVA® *Gen3 Ultra lightweight robot* (Kinova inc., 2022), and a PC computer equipped with the KINOVA® Kortex™ software and the UBUNTU® operating system with the PREEMPT_RT patches. A schematic view of the laboratory test–bed is shown in Fig. 4.

For both validation scenarios the same parameters and conditions were assumed. A path in a shape of a helix was followed. The helix is described with the following equation (Oprea, 2007)

$$r(s) = \begin{pmatrix} a\cos\frac{s}{c} & a\sin\frac{s}{c} & \frac{bs}{c} \end{pmatrix}^T, \qquad (19)$$

[1]An animation of the simulation results and a video of the experiment are available on the webpage: https://kcir.pwr.edu.pl/~fdyba/ICINCO/.

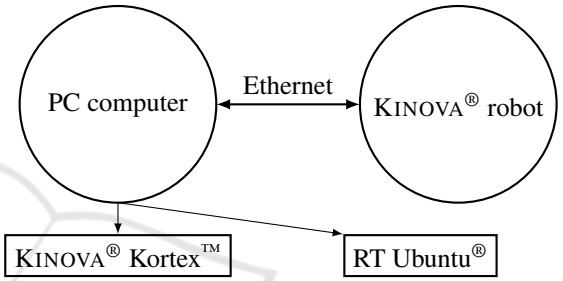

Figure 4: Scheme of the experimental test–bed.

where it was assumed that $a = 0.5$, $b = 0.05$ and $c = \sqrt{a^2 + b^2}$. Moreover, the desired velocity profile along the path was assumed as $\dot{s}_d = 0.25\text{m/s}$. The manoeuvre lasted 30s. The control gains were equal to $K_k = \text{diag}_{3\times3}\{50\}$, $K_p = \text{diag}_{7\times7}\{5\}$, and $K_d = \text{diag}_{7\times7}\{5\}$. The radius of the dead zone was equal to $\lambda = 0.1$ and the initial value of the gain adaptation was chosen as $K(0) = 1$. Finally, the chosen initial configuration of the manipulator was equal in degrees to

$$q_0 = \begin{pmatrix} -1.34 \\ 87.65 \\ -3.02 \\ 108.60 \\ -1.54 \\ -106.32 \\ -87.16 \end{pmatrix}. \qquad (20)$$

The manipulator in the initial state is presented in Fig. 5.

The following figures show graphs comparing simulation and experimental results. Firstly, in Fig. 6 the desired path is compared with the path performed in both versions of the test. There are no observable differences between the desired and executed paths. However, at the beginning a slight deviation from the given path may be noticed. For the real manipulator the disturbance is even more significant. It may result

Figure 5: KINOVA® manipulator in the initial configuration.

from some mechanical issues independent from the control algorithm performance. The disturbance was quickly compensated by the control system in both cases and the manipulator successfully followed the desired path.

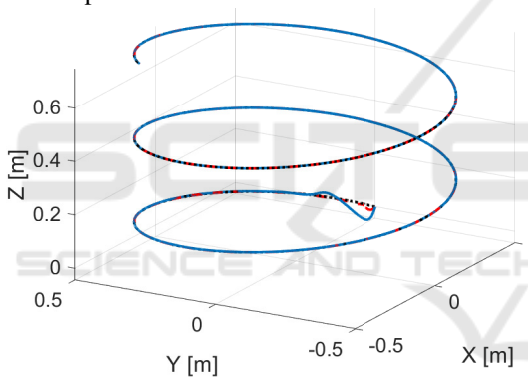

Figure 6: Path performed by the manipulator (blue solid —— Experiment, red dashed - - - Simulation, black dotted ····· Desired).

In Fig. 7 path following errors are shown. Indeed, they reveal the greater deviation measured for the physical object at the beginning of the manoeuvre. It is noteworthy that the obtained precision of the motion is satisfactory. Although some noise oscillations may be observed for the experimental case, the error signals are of the order $(0.1-1)$mm. It might result from the limited precision of mechanical elements or sensors. Nevertheless, such precision is sufficient for autonomous path following or grasping manoeuvres.

Furthermore, Figs. 8 and 9 present errors of following velocity profiles in the large and small joints (Kinova inc., 2022), respectively. It can be observed that errors for the experimental case are higher at the beginning of the manipulator movement. It results from the mentioned above disturbances. In addition, the transient state lasts longer. Nonetheless, after a short period of time there are no significant differences between simulation and experimental results. Moreover, all velocity profile following errors tend towards the bounds resulting from the chosen control parameters. After a certain time the values are kept within the bounds. Hence, the end-effector correctly follows positions defined by the helix equation (19).

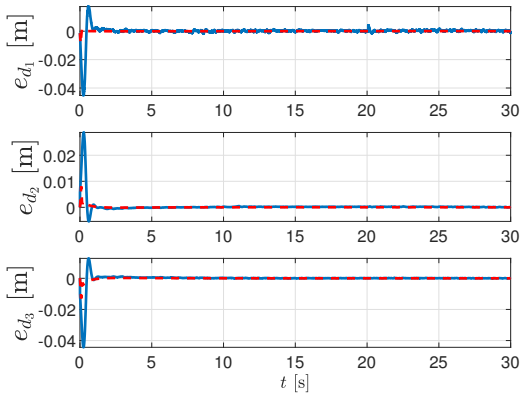

Figure 7: Path following erros $\boldsymbol{e_d}$ (blue solid —— Experiment, red dashed - - - Simulation).

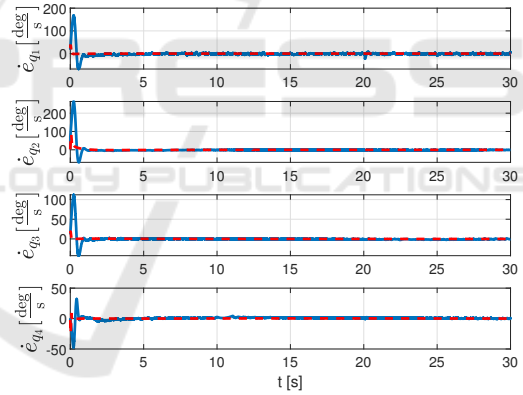

Figure 8: Velocity profile following erros $\dot{\boldsymbol{e}}_{\boldsymbol{q}}$ for large joints (blue solid —— Experiment, red dashed - - - Simulation).

Finally, Figs. 10 and 11 present control torques generated for the large and small joints, respectively. In the transient state the values generated for the physical manipulator are higher, although the signal changes are not as rapid as for the simulation case. In addition, some subtle differences may be observed during the whole manoeuvre in every joint, especially in the first one. It may result from the fact that in the simulation case some factors were neglected, e.g. friction forces. They appeared, though, in the experimental case. However, despite the simplified model in the simulation case, the obtained results do not differ significantly and the trend of the measurements is maintained.

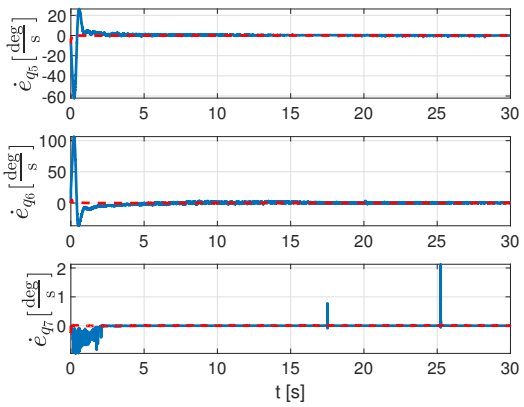

Figure 9: Velocity profile following erros $\dot{e}_q$ for small joints (blue solid —— Experiment, red dashed - - - Simulation).

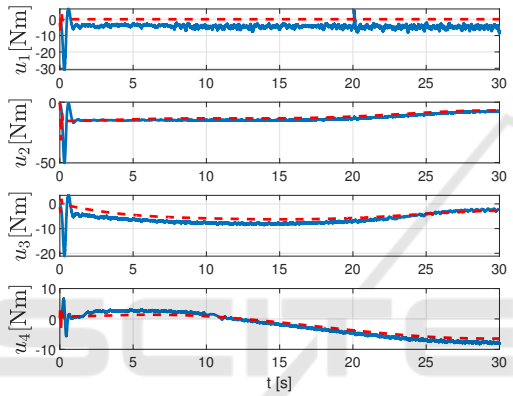

Figure 10: Control torques u for large joints (blue solid —— Experiment, red dashed - - - Simulation).

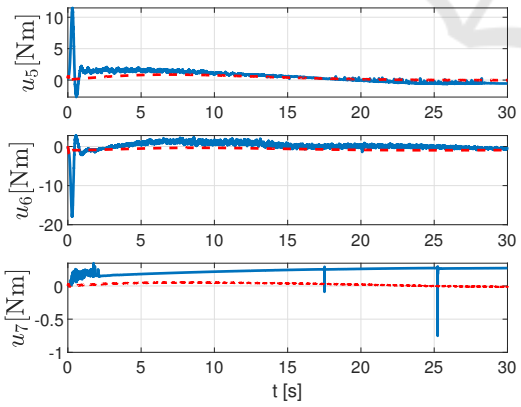

Figure 11: Control torques u for small joints (blue solid —— Experiment, red dashed - - - Simulation).

All in all, the obtained experimental measurements correspond with the simulation results. In spite of the minor differences resulting from some mechanical or implementation issues which arose on the laboratory test–bed, the path was tracked correctly by the real KINOVA® manipulator. Hence, it can be concluded that the presented path following algorithm is suitable for practical applications.

6 CONCLUSIONS

In the paper the path following algorithm has been presented. It is based on two main aspects:

- the non-orthogonal Serret–Frenet parametrization used for deriving the robot equations with respect to the desired path (equations have the form of a non-holonomic constraint);
- the backstepping integrator algorithm used for the design of the control law.

The considered description is valid globally in every point of a feasible path. Satisfying the equations resulting from the Serret–Frenet parametrization guarantees correct path following. However, it can be performed only via the manipulator dynamics.

As a consequence, the control system has a cascaded structure and the backstepping algorithm is used to design two stages of the control cascade. The proposed dynamic control law (the λ-tracking algorithm) did not require any knowledge of the dynamics parameters. However, the adaptively tuned control gain guaranteed that the error converge to the predefined region. This property allowed the robot to successfully follow the path.

The presented algorithm has been validated with the simulation and experimental studies. The simulation results were more precise. In the experiment a disturbance at the beginning of the manoeuvre and some noise in the measurements were observed. The differences may result from some mechanical issues, delays in the transmission between the computer and the manipulator on the experimental test–bed, or simplifications of the simulation model. Nonetheless, the discrepancies were not crucial for the successful completion of the control task — the desired path was followed correctly. The gathered experimental measurements confirmed that the designed algorithm can be successfully applied to practical problems.

The results of the experiments indicate further research directions. Firstly, the motion precision may be improved. Although the achieved accuracy is satisfactory for autonomous path following or even some grasping manoeuvres, it might not be sufficient for some operations such as milling. Thus, identification of the dynamic structure of the manipulator may be conducted in order to use a controller based on the fully-known robot dynamics, or to consider some neglected effects such as friction forces.

Secondly, it may be observed that the end-effector

orientation with respect to the Serret–Frenet frame changes during the manoeuvre. Such a behaviour may be unfavourable in grasping processes. Hence, not only the position control, but also the orientation control should be taken into consideration.

Finally, the control constraints could be taken into account in the control law. It will be especially important if the end-effector is outside the path in the initial state. It may prevent the control system from rapid reactions in the transient state.

REFERENCES

Cholewiński, M. and Mazur, A. (2019). Path tracking by the nonholonomic mobile manipulator. In *2019 12th International Workshop on Robot Motion and Control (RoMoCo)*, pages 203–208, Poznan, Poland.

Domski, W. and Mazur, A. (2018). Path tracking with orthogonal parametrization for a satellite with partial state information. In *Proceedings of the 15th International Conference on Informatics in Control, Automation and Robotics*, volume 2, pages 252–257, Porto, Portugal.

Dyba, F. and Mazur, A. (2023). Comparison of curvilinear parametrization methods and avoidance of orthogonal singularities in the path following task. *Journal of Automation, Mobile Robotics and Intelligent Systems. (In press)*.

Encarnação, P. and Pascoal, A. (2000). 3D path following for autonomous underwater vehicle. In *Proceedings of the 39th IEEE Conference on Decision and Control*, pages 2977–2982, Sydney, NSW, Australia.

Hung, N., Rego, F., Quintas, J., Cruz, J., Jacinto, M., Souto, D., Potes, A., Sebastiao, L., and Pascoal, A. (2023). A review of path following control strategies for autonomous robotic vehicles: Theory, simulations, and experiments. *Journal of Field Robotics*, 40(3):747–779.

Kinova inc. (2022). Kinova Gen3 Ultra lightweight robot user guide r8. Technical Report EN-UG-014-r8-202210, Quebeck, Canada.

Krstić, M., Kanellakopoulos, I., and Kokotović, P. V. (1995). *Nonlinear and Adaptive Control Design*. John Wiley & Sons, Inc., New York, USA.

Liao, Y.-L., Zhang, M.-J., and Wan, L. (2015). Serret–Frenet frame based on path following control for underactuated unmanned surface vehicles with dynamic uncertainties. *Journal of Central South University*, 22:214–223.

Lugo-Cárdenas, I., Salazar, S., and Lozano, R. (2017). Lyapunov Based 3D Path Following Kinematic Controller for a Fixed Wing UAV. *IFAC-PapersOnLine*, 50(1):15946–15951. 20th IFAC World Congress.

Mazur, A. and Cholewiński, M. (2016). Implementation of factitious force method for control of 5R manipulator with skid-steering platform REX. *Bulletin of the Polish Academy of Sciences Technical Sciences*, 64(No. 1):71–80.

Mazur, A. and Dyba, F. (2023). The Non-orthogonal Serret–Frenet Parametrization Applied to the Path Following Problem of a Manipulator with Partially Known Dynamics. *Archives of Control Sciences*, 33(2):339–370.

Mazur, A. and Płaskonka, J. (2012). The Serret–Frenet parametrization in a control of a mobile manipulator of (nh, h) type. *IFAC Proceedings Volumes*, 45(22):405–410. 10th IFAC Symposium on Robot Control.

Mazur, A., Płaskonka, J., and Kaczmarek, M. (2015). Following 3D paths by a manipulator. *Archives of Control Sciences*, 25(1):117–133.

Mazur, A. and Schmid, C. (2000). Adaptive λ-tracking for rigid manipulators. In Morecki, A., Bianchi, G., and Rzymkowski, C., editors, *Romansy 13. Theory and practice of robots and manipulators.*, pages 103–112, Vienna. Springer Vienna.

Mazur, A. and Szakiel, D. (2009). On path following control of nonholonomic mobile manipulators. *International Journal of Applied Mathematics and Computer Science*, 19(4):561–574.

Micaelli, A. and Samson, C. (1993). Trajectory tracking for unicycle-type and two-steering-wheels mobile robots. In *Technical Report No. 2097*, Sophia-Antipolis.

Michałek, M. M. and Gawron, T. (2018). VFO path following control with guarantees of positionally constrained transients for unicycle-like robots with constrained control input. *Journal of Intelligent and Robotic Systems: Theory and Applications*, 89(1-2):191 – 210.

Morro, A., Sgorbissa, A., and Zaccaria, R. (2011). Path following for unicycle robots with an arbitrary path curvature. *IEEE Transactions on Robotics*, 27(5):1016–1023.

Oprea, J. (2007). *Differential Geometry and Its Applications*. Prentice Hall, Washington, Cleveland State University.

Płaskonka, J. (2013). Different kinematic path following controllers for a wheeled mobile robot of (2,0) type. *Journal of Intelligent & Robotic Systems*, 77:481–498.

Qu, Z. and Dorsey, J. (1991). Robust tracking control of robots by a linear feedback law. *IEEE Transactions on Automatic Control*, 36(9):1081–1084.

Rokonuzzaman, M., Mohajer, N., Nahavandi, S., and Mohamed, S. (2021). Review and performance evaluation of path tracking controllers of autonomous vehicles. *IET Intelligent Transport Systems*, 15(5):646–670.

Selig, J. M. (2005). *Geometric Fundamentals of Robotics*. Springer New York, NY, 2nd edition.

Siciliano, B. and Khatib, O. (2007). *Handbook of Robotics*. Springer-Verlag, Berlin, Heidelberg.

Spong, M. and Vidyasagar, M. (1991). *Robot Dynamics and Control*. John Wiley & Sons, Inc., New York.